LETTERS

A strong, highly-tilted interstellar magnetic field near the Solar System

M. Opher[1], F. Alouani Bibi[1], G. Toth[2], J. D. Richardson[3], V. V. Izmodenov[4] & T. I. Gombosi[2]

Magnetic fields play an important (sometimes dominant) role in the evolution of gas clouds in the Galaxy, but the strength and orientation of the field in the interstellar medium near the heliosphere has been poorly constrained. Previous estimates of the field strength range from 1.8–2.5 μG and the field was thought to be parallel to the Galactic plane[1] or inclined by 38–60° (ref. 2) or 60–90° (ref. 3) to this plane. These estimates relied either on indirect observational inferences or modelling in which the interstellar neutral hydrogen was not taken into account. Here we report measurements of the deflection of the solar wind plasma flows in the heliosheath[4] to determine the magnetic field strength and orientation in the interstellar medium. We find that the field strength in the local interstellar medium is 3.7–5.5 μG. The field is tilted ~20–30° from the interstellar medium flow direction (resulting from the peculiar motion of the Sun in the Galaxy) and is at an angle of about 30° from the Galactic plane. We conclude that the interstellar medium field is turbulent or has a distortion in the solar vicinity.

The local interstellar medium magnetic field (B_{ISM}) is one of the key elements that control the interaction between the Solar System and the interstellar medium. Determining its strength and orientation is crucial because B_{ISM} affects the shape of the Solar System and the filtration of particles that stream into the Solar System from the interstellar medium. However, until the Voyager spacecraft crosses the heliopause, we cannot directly measure the orientation or strength of B_{ISM}.

Previous work estimated the orientation and intensity of B_{ISM}, but with large uncertainties. Measurements of the polarization of light from nearby stars[1] suggest that the average field over spatial scales of parsecs is parallel to the Galactic disk, but gives no information on the local field direction. The backscattered solar Lyman-α radiation[2] gave a field direction inclined 38–60° with respect to the Galactic plane with the angle between the velocity of the interstellar medium and magnetic field assumed to be 30–60°. This method relies on the assumption that B_{ISM} is in a plane defined by the interstellar H and He flow directions as they penetrate the Solar System. However, recent studies have shown that this assumption may not be valid[5].

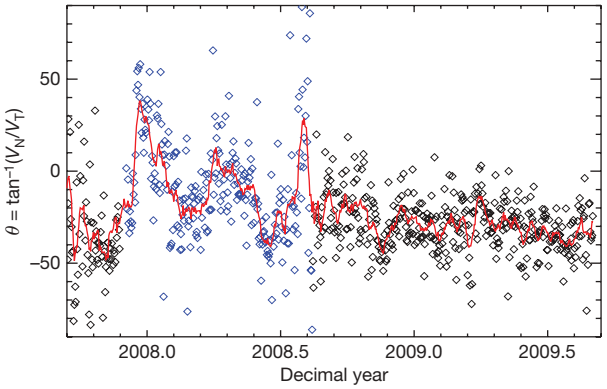

Figure 1 | Flows in the heliosheath as measured by Voyager 2. The flow angle $\theta = \tan^{-1}(V_N/V_T)$ is shown from day 277 of 2007 to day 245 of 2009 as measured by Voyager 2 in the R–T–N coordinate system. The horizontal axis shows the time in decimal years (day/365) from 2007–2009. The period between 2007.95 and 2008.62 (blue points) seems to be dominated by transients that may be driven by interactions between the fast and slow solar wind. We model the steady-state heliosphere and thus remove this region to calculate the average flow angle in the heliosheath. The average angle θ is $-29^\circ \pm 1.0^\circ$. The red line shows 11-day running averages of the angles.

The deflection of the H from the He flow direction is affected both by the orientation and by the strength of B_{ISM}. The same observed average deflection can be produced by different orientations and intensities of B_{ISM}. Previous studies do not constrain the strength of the field. We previously[3,6,7] derived the strength and orientation of the B_{ISM} from a numerical model constrained by Voyager 1 and 2 particle streaming and radio observations . This model did not include neutral H atoms, so it underestimated the strength of the interstellar magnetic field and had large uncertainties in the field direction[8,9].

Here we constrain the orientation and strength of B_{ISM} using a new data set, the heliosheath flows obtained from Voyager 2 measurements.

Table 1 | Definitions of the parameters used

α	Angle between the local interstellar magnetic field and interstellar wind (see also Fig. 3 inset)
β	Angle between the solar equatorial plane and the plane defined by the interstellar magnetic field and the interstellar wind
θ	$\tan^{-1}(V_N/V_T)$; the angle describing the flow deflection in the heliosheath
θ_1	Angle between the shock normal n and the Sun-centred radius vector
ϕ_1	Angle measured between the tangential direction T and the projection of n in the N–T plane (see Supplementary Information for a diagram)
V_S	Shock velocity
R_{TS}	Distance of the termination shock to the Sun
V_R	Radial velocity in the R–T–N coordinate system, that is, a local cartesian system centred at the spacecraft. R is radially outward from the Sun, T is in the plane of the solar equator and positive in the direction of solar rotation, and N completes a right-handed system
V_N	Normal velocity in the R–T–N coordinate system
V_T	Tangential velocity in the R–T–N coordinate system

[1]George Mason University, 4400 University Drive, Fairfax, Virginia 22030, USA. [2]Center for Space Environment Modeling, University of Michigan, Ann Arbor, Michigan 48109, USA. [3]Kavli Institute for Astrophysics and Space Research, Massachusetts Institute of Technology, 37-655, 77 Massachusetts Avenue, Cambridge, Massachusetts 02139, USA. [4]Lomonosov Moscow State University, Space Research Institute (IKI) and Institute for Problems in Mechanics, Russian Academy of Science, 84/32 Profsoyuznaya Street, Moscow 117997, Russia.

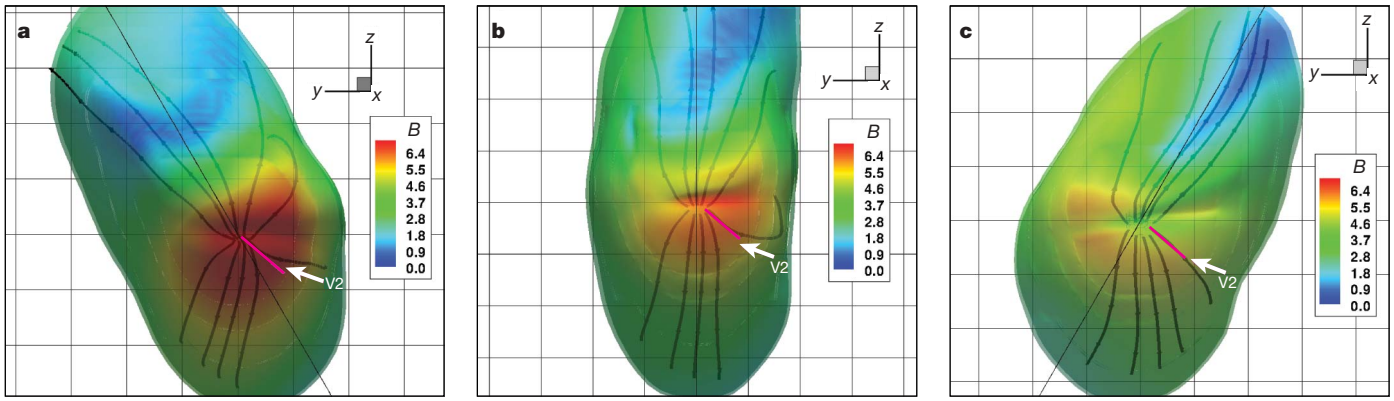

Figure 2 | Flows in the heliosheath for different B_{ISM} directions. The shapes of the heliopause are shown for $B_{ISM} = 4.4\,\mu G$, $\alpha = 45^\circ$ and β equal to 60° (**a**), 90° (**b**) and 120° (**c**). The colours indicate the total magnetic field strength (in microgauss) and are shown on the iso-surface of the heliopause defined for $\ln T = 11.5$, where T is the temperature. The viewpoint is from the $+x$ direction. The streamlines show qualitatively the difference in flow patterns in the heliosheath. The interstellar wind is along the x-axis, the solar rotation axis is along the z-axis and the y-axis completes the right-handed coordinate system. In this coordinate system, the Voyager 2 trajectory is shown by the pink lines labelled V2. The Voyager 2 ecliptic latitude and longitude are −31.2° and 213.4° respectively, neglecting the 7.25° tilt of the solar equator with respect to the ecliptic plane. The heliopause surfaces and flows for the $\beta = 60^\circ$ (**a**) and $\beta = 120^\circ$ (**b**) orientations are almost mirror images. The heliopause is asymmetric, both in the north–south and in the east–west directions, and has a plane of symmetry approximately parallel to the plane of the local B_{ISM}. The intensity of the magnetic field outside the heliopause is larger in the southern solar hemisphere rather than in the northern solar hemisphere (**a**) owing to the slowing-down of the plasma flow.

The heliosheath flow angle $\theta = \tan^{-1}(V_N/V_T)$ depends on the interstellar medium magnetic field. (The coordinate system is defined in Table 1.) Figure 1 shows the flow angle θ in the heliosheath at Voyager 2. This dependence of the flow angle on the magnetic field orientation can be seen qualitatively in Fig. 2, which shows the flows predicted by a three-dimensional magnetohydrodynamic model with five fluids (one ionized and four neutral H fluids; see description in Supplementary Information).

The orientation of the interstellar magnetic field is defined by the angles α and β, where α is the angle between the interstellar magnetic field and the interstellar wind and β is the angle between the solar equator and the plane defined by the interstellar magnetic field and the interstellar wind (see inset in Fig. 3). (The Local Standard of Rest is the mean motion of the stars and gas in the solar neighbourhood in rotation around the Galactic centre. The Sun moves relative to the Local Standard of Rest at 13.4 km s^{-1} in the direction of Galactic rotation, −9 km s^{-1} in the radial direction, and 3.7 km s^{-1} in the vertical direction. The cloud of material that surrounds the Sun moves in the Local Standard of Rest in a nearly perpendicular motion. The result of these two motions is that we observe interstellar material flowing towards the Sun, called the interstellar wind. We use the interstellar wind direction to define the x-axis of our model (see Supplementary Fig. 4).) We constrain the value of α by comparing the observed distances of the termination shock from the Sun in the Voyager 1 and Voyager 2 directions[10,11] to the model results (Table 2) and find that values of α between 20° and 30° fit the data. The magnitude of B_{ISM} must be between 3.7 μG and 5.5 μG to match the observed termination shock crossing distances. We note that other work found α to be 15–20° and the magnitude to be about 4 μG, but these studies did not take into account the interplanetary magnetic field[12]. We constrain the value of β by comparing the measured and simulated flow velocities. Figure 3 shows the dependence of β on the flow angle for several values of α. For $\alpha = 20$–30°, as β increases the predicted flow angle θ agrees better with the measured angle. β has to be less than 90° due to magnetic connectivity[3], so β near 90° (or about 30° from the Galactic plane) gives the best fit to the observations.

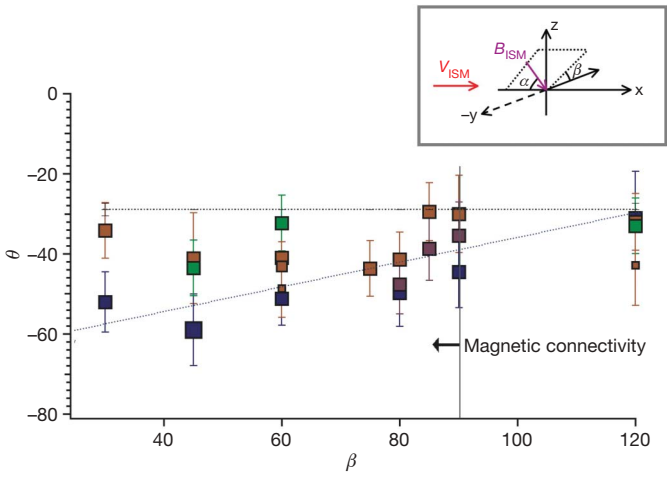

Figure 3 | Modelled flows as a function of the B_{ISM}. The flow angle $\theta = \tan^{-1}(V_N/V_T)$ is shown as a function of the B_{ISM} orientation. Flow angles for $\alpha = 20^\circ$, 30°, 45° and 60° are shown in blue, purple, brown and green, respectively. The size of the squares corresponds to the intensity of B_{ISM} from 2.5–5.5 μG. The model flow angle θ was estimated using all the points within two cells of resolution (or 6 AU) of the Voyager 2 trajectory (see Supplementary Information). The error bars are the root mean square of all the values. The observed flow angle $\theta = -29^\circ \pm 1.0^\circ$ is shown by the dotted line. The blue dashed line illustrates the dependence of the flow angle on β for $\alpha = 20$–30°. The inset shows the orientation of α and β in the model coordinate systems (for more details see Table 1). The velocity of the interstellar wind is indicated by the label V_{ISM}.

We analyse the effects of non-stationarity and numerical resolution on our estimates of the magnetic field orientation and find them to be negligible. The effects of the non-stationarity of the shock can be obtained from the theoretical predictions of θ for a three-dimensional magnetized moving shock given by the Rankine–Hugoniot conditions and described by the angles θ_1 and ϕ_1 (for definitions see Table 1). The termination shock at the time of the Voyager 2 crossing had, on average, $\theta_1 = 15^\circ$, $\phi_1 = 165^\circ$ and $V_S = 88.09$ km s^{-1}, where V_S is the shock velocity (see Supplementary Information for more details). Using the Rankine–Hugoniot conditions with these values for θ_1 and ϕ_1, we estimate that the dependence of θ (the orientation of the flow which constrains the orientation of the magnetic field) on the shock velocity V_S is less than 0.1°. In the Supplementary Information we show that the effect of numerical resolution is also small (less than 8°). We show that the obliquity of the shock given by θ_1 and ϕ_1 depends on the interstellar magnetic field (see Supplementary Information for details).

These results show that the local B_{ISM} orientation with respect to the Galactic plane is different from that determined from ground-based

Table 2 | Termination shock distances at Voyager 1 and 2 as a function of B_{ISM}

B (μG)	β (°)	α (°)	R_{TS}(V1) (AU)	R_{TS}(V2) (AU)	R_{TS}(V2) − R_{TS}(V1) (AU)
4.4	30	20	88.7 ± 3.6	79.8 ± 2.3	8.9
4.4	60	20	90.3 ± 4.0	81.2 ± 2.7	9.1
4.4	80	20	94.1 ± 4.8	85.8 ± 2.7	8.3
4.4	120	20	94.2 ± 3.4	92.9 ± 4.7	1.3
5.5	45	20	84.6 ± 3.6	72.4 ± 2.6	12.2
4.4	80	30	88.5 ± 3.8	79.3 ± 2.4	9.2
4.4	85	30	88.8 ± 3.8	82.6 ± 4.9	6.2
4.4	90	30	89.2 ± 4.2	81.1 ± 2.5	8.1
2.5	60	45	89.1 ± 3.8	85.3 ± 3.0	3.8
3.7	60	45	82.7 ± 3.5	70.7 ± 3.4	12.0
4.4	60	45	76.6 ± 1.5	67.8 ± 2.3	8.8
4.4	75	45	78.1 ± 2.0	70.2 ± 2.4	7.9
4.4	80	45	79.2 ± 2.6	71.8 ± 1.9	7.4
4.4	85	45	80.2 ± 1.9	74.5 ± 2.6	7.8
4.4	120	45	80.3 ± 3.0	78.9 ± 2.6	1.9
4.4	30	45	73.1 ± 1.9	67.1 ± 2.0	6.0
4.4	45	45	74.4 ± 2.0	68.4 ± 2.6	6.0
4.4	90	45	80.4 ± 1.9	73.3 ± 2.0	7.1
4.4	120	60	72.9 ± 1.9	67.2 ± 2.2	5.7
4.4	60	60	73.0 ± 2.0	67.5 ± 2.2	5.5

The error bars in the termination shock distances R_{TS} are the average of the upstream and downstream distances. The angle α is the dominant factor in determining the distance of the termination shock to the Sun and the asymmetry between Voyager 1 (V1) and Voyager 2 (V2), R_{TS}(V1) − R_{TS}(V2) (in astronomical units, AU). Models that take into account the motion of the shock[22,23] estimate an asymmetry of 7 AU between the termination shock distances in the Voyager 1 and 2 directions. To reproduce the observed asymmetry of 7 AU, B_{ISM} must be >3.7 μG. To reproduce the distances R_{TS}(V1) = 91 AU and R_{TS}(V2) = 83.7 AU, the angle α has to be 20–30°.

measurements, which determine the average field orientation over large distances[1]. This difference could be a result of turbulence in the interstellar medium[13,14] which could cause the local magnetic field direction to differ dramatically from that of the large-scale field. This difference could also be a consequence of local distortion of the magnetic field in the solar vicinity[15]. Within 100–200 pc from the Sun, the interstellar gas is embedded in the Local Bubble[16], a huge region of hot tenuous plasma which contains small, cooler, denser clouds such as the Local Interstellar Cloud (also called the Local Cloud), which envelops the Sun. Collisions between the Local Cloud and other cooler, denser clouds in the Local Bubble, such as the G cloud[17], could cause such a distortion. Theories for the creation of the Local Cloud suggest that the magnetic fields are strong, of the order of 4–7 μG (ref. 18).

For a magnetic field strength in the Local Cloud of 4 μG, which we report here, the magnetic pressure would be $P_B/k \approx 4{,}500\ \mathrm{K\,cm^{-3}}$ (where k is the Boltzmann constant), almost twice the Local Cloud thermal pressure of $P_{th}/k \approx 2{,}500\ \mathrm{K\,cm^{-3}}$ (refs 19, 20). If this magnetic field strength were representative of the local field over a scale of about 10 pc, the magnetic energy density could dominate the energy budget in the Local Cloud[20,21].

Received 18 May; accepted 6 October 2009.

1. Frisch, P. C. LISM structure-fragmented superbubble shell? *Space Sci. Rev.* **78,** 213–222 (1996).
2. Lallement, R. *et al.* Deflection of the interstellar neutral hydrogen flow across the heliospheric interface. *Science* **307,** 1447–1449 (2005).
3. Opher, M., Stone, E. C. & Gombosi, T. I. The orientation of the local interstellar magnetic field. *Science* **316,** 875–878 (2007).
4. Richardson, J. D. *et al.* Cool heliosheath plasma and deceleration of the upstream solar wind at the termination shock. *Nature* **454,** 63–66 (2008).
5. Pogorelov, N. V. & Zank, G. P. The direction of the neutral hydrogen velocity in the inner heliosphere as a possible interstellar magnetic field compass. *Astrophys. J.* **636,** L161–L164 (2006).
6. Opher, M., Stone, E. C. & Liewer, P. C. The effects of a local interstellar magnetic field on Voyager 1 and 2 observations. *Astrophys. J.* **640,** L71–L74 (2006).
7. Opher, M., Richardson, J. C., Toth, G. & Gombosi, T. I. Confronting observations and modeling: the role of the interstellar magnetic field in Voyager 1 and 2 asymmetries. *Space Sci. Rev.* **143,** 43–55 (2009).
8. Pogorelov, N. V., Stone, E. C., Florinski, V. & Zank, G. P. Termination shock asymmetries as seen by the Voyager spacecraft: the role of the interstellar magnetic field and neutral hydrogen. *Astrophys. J.* **668,** 611–624 (2007).
9. Pogorelov, N. V., Heerikhuisen, J. & Zank, G. P. Probing heliospheric asymmetries with an MHD-kinetic model. *Astrophys. J.* **675,** L41–L44 (2008).
10. Stone, E. C. *et al.* An asymmetric solar wind termination shock. *Nature* **454,** 71–74 (2008).
11. Stone, E. C. *et al.* Voyager 2 explores the termination shock region and the heliosheath beyond. *Science* **309,** 2017–2020 (2005).
12. Izmodenov, V. V. Local interstellar parameters as they are inferred from analysis of observations inside the heliosphere. *Space Sci. Rev.* **143,** 139–150 (2009).
13. Minter, A. H. & Spangler, S. R. Observation of turbulent fluctuations in the interstellar plasma density and magnetic field on spatial scales of 0.01 to 100 parsecs. *Astrophys. J.* **458,** 194–214 (1996).
14. Jokipii, J. R. Our interstellar neighborhood. *Science* **307,** 1424–1425 (2007).
15. Frisch, P. C. *et al.* The galactic environment of the Sun: interstellar material inside and outside the heliosphere. *Space Sci. Rev.* **146,** 235–273 (2009).
16. Linsky, J. L. Solving the mysteries of the diffuse interstellar medium with high-resolution UV spectroscopy. *Astrophys. Space Sci.* **320,** 85–90 (2009).
17. Redfield, S. & Linsky, J. The structure of the local Interstellar Medium. IV. Dynamics, morphology, physical properties, and implications of cloud-cloud interactions. *Astrophys. J.* **673,** 283–314 (2008).
18. Cox, D. & Helenius, L. Flux-tube dynamics and a model for the origin of the local fluff. *Astrophys. J.* **583,** 205–228 (2003).
19. Jenkins, E. B. & Tripp, T. M. The distribution of thermal pressures in the interstellar medium from a survey of CI fine-structure excitation. *Astrophys. J. Suppl. Ser.* **137,** 297–340 (2001).
20. Shelton, R. *et al.* The local bubble debate. Report from sessions 1 and 3. *Space Sci. Rev.* **143,** 303–309 (2009).
21. Jenkins, E. B. Pressure and ionization balances in the circum-heliospheric interstellar medium and the local bubble. *Space Sci. Rev.* **143,** 205–216 (2009).
22. Izmodenov, V. V., Malama, Y. G. & Ruderman, M. S. Modeling of the outer heliosphere with the realistic solar cycle. *Adv. Space Res.* **41,** 318–324 (2008).
23. Richardson, J. D., Liu, Y. & Wang, C. Solar wind structure in the outer heliosphere. *Adv. Space Res.* **41,** 237–244 (2008).

Supplementary Information is linked to the online version of the paper at www.nature.com/nature.

Acknowledgements We thank the staff at NASA Ames Research Center for the use of the Columbia supercomputer. M.O. and F.A.B. acknowledge the support of NASA and the National Science Foundation. J.R. is supported by the Voyager project. V.V.I. acknowledges the support of the Russian Agency of Science and the Dynastia Foundation. We thank E. C. Stone and R. Shelton for suggestions and comments.

Author Contributions M.O. ran the models and wrote the paper. F.A.B. performed the R-H calculations, the model flow calculations, and participated in the writing of the paper. J.D.R. analysed the plasma data. G.T. helped implement the five-fluid magnetohydrodynamic model. V.V.I. assisted in the theoretical discussions, including solar cycle effects. T.I.G. provided assistance with the global magnetohydrodynamic model.

Author Information Reprints and permissions information is available at www.nature.com/reprints. Correspondence and requests for materials should be addressed to M.O. (mopher@gmu.edu).